JOURNAL OF CATALYSIS 157, 388–395 (1995)

Monomolecular Conversion of Light Alkanes over H–ZSM-5

Thomas F. Narbeshuber,* Hannelore Vinek,† and Johannes A. Lercher*

*Christian Doppler Laboratory for Heterogeneous Catalysis, Department of Chemical Technology, University of Twente, P.O. Box 217, 7500 AE Enschede, The Netherlands; and †Institute of Physical Chemistry, Technical University of Vienna, Getreidemarkt 9, A-1060 Vienna, Austria

Received January 19, 1995; revised July 12, 1995; accepted August 4, 1995

The monomolecular conversion of light *n*-alkanes (propane to *n*-hexane) over H–ZSM-5 was investigated between 723 and 823 K. The rates and energies of activation of the individual reactions were determined and a kinetic model for the conversion is presented. The results suggest that carbonium ions are intermediates for all primary reactions. Depending upon the nature of the carbonium ion in the transition state, three parallel primary reactions were identified, leading to hydrogen exchange, dehydrogenation, and cracking. With increasing size of the *n*-alkane, the rate of reaction increases due to the increase in the adsorption constant of the hydrocarbon. The true energies of activation are independent of the hydrocarbon chain length and the position of the carbon–carbon bond to be cleaved.

INTRODUCTION

Because of its vital importance in the petroleum industry, cracking of hydrocarbons has been of remarkable interest in the academic and the industrial communities over the past decades. This is well documented in several review articles (e.g., 1–6). The characterization of the active components of cracking catalysts, the understanding of the complex reaction network occurring during cracking of industrial feed stocks, and the use of test reactions for the evaluation of catalyst performance were the focus of interest. The use of small alkanes as probe reactants for the evaluation of catalytic properties of cracking catalysts has been hotly debated (7–11) and quite strong disagreement as to the best suited molecule still exists. It was thus our aim to compare the detailed kinetics of catalyzed reactions of light *n*-alkanes (propane to *n*-hexane), i.e., cracking, dehydrogenation, and hydrogen exchange, in order to prove the possibilities and limitations of these reactions with respect to catalyst characterization. In this communication, we will mainly focus on cracking and discuss hydrogen exchange reactions and dehydrogenation only as needed to explain the possible product distributions.

Two pathways of acid-catalyzed cracking of saturated hydrocarbons are commonly accepted: (i) the classical bimolecular carbenium ion chain mechanism (β-cracking) which involves the activation of the *n*-alkane via hydride transfer to a surface-bound carbenium ion followed by β-scission of this newly formed carbenium ion (10–14) and (ii) the monomolecular (protolytic cracking) pathway which involves the formation of pentacoordinated carbonium ions (6, 11) and cleavage of the carbon–carbon bond adjacent to the carbon atom bearing the positive charge. In the first case, the rate-determining step of the reaction is concluded to be the hydride transfer following the initial generation of the carbenium ion; in the latter case the rate is determined by carbonium ion formation (generated by addition of protons to the saturated hydrocarbons) or their subsequent decay. The prevalance of one of the two mechanisms is governed by the reaction temperature and the surface concentration of the reactants (determined by temperature, reactant pressure, and the concentration of acid sites) (11).

For the present study, the reaction conditions were chosen so that monomolecular reactions prevailed for the primary conversion of the hydrocarbons. The individual primary reaction steps and the contribution of the secondary reactions will be discussed. A reaction scheme of *n*-alkane cracking over H–ZSM-5 and the energetics of the observed processes will be presented.

EXPERIMENTAL

H–ZSM-5 (obtained from Mobil) with a Si/Al ratio of 35 and an average particle size of 1 μm was used for the present investigation. The concentration of Brønsted acid sites was determined to be 4.2×10^{-4} mol/g by temperature-programmed desorption of pyridine and ammonia. The experimental conditions for these measurements and detailed information about the physicochemical properties are documented in Ref. (15). All acid sites were found to be accessible for reactant molecules as probed by *in situ* IR measurements of the sorption of linear alkanes (C_3–C_6) at 300 K. The BET surface area of the material was 300 m^2/g, and the micropore volume was 0.06 cm^3/g. The ZSM-5 sample did not contain detectable amounts of extra lattice alumina species (determined by ^{27}Al NMR) or Na^+ cations

0021-9517/95 $12.00

(determined by EDAX). The phase purity of the material was checked by XRD.

The catalytic conversion of the linear hydrocarbons between 723 and 823 K was carried out in a tubular flow reactor with an inner diameter of 5 mm operated under stationary conditions. Typical catalyst weights varied from 0.005 to 0.05 g. For catalyst weights exceeding 0.02 g, quartz was applied as dilutant to minimize the pressure drop over the catalyst bed. The catalyst was activated in a stream of air by increasing the temperature (10 K/min) to 873 K and maintaining this temperature for 1 h. Then, the sample was cooled to reaction temperature in a stream of He. The reactants were used either premixed with the carrier gas (propane 10%, and *n*-butane 2% in He 5.0) or added to the He carrier stream via a saturator or a syringe pump (*n*-pentane and *n*-hexane). The partial pressures were varied from 0.1 to 10 kPa. Flow rates were adjusted between 10 and 100 ml/min to maintain differential reaction conditions.

Data reported here correspond to steady state values taken between 15 and 60 min time on stream. Catalyst deactivation did not take place under the experimental conditions chosen, as shown by the transient response technique (see Ref. 16).

Correlation coefficients of linear dependencies reported in the present communication (E_A, dr/dp) were in all cases better than 0.99. The energies of activation have a maximum standard deviation of 7%.

The products were separated by means of gas chromatography (HP-5890 II) using an Al_2O_3/KCl capillary column and analyzed with a flame ionization detector and a mass spectrometer (HP-5971A). The absence of thermal cracking was confirmed with blank experiments.

REACTION PATHWAYS

In order to establish the rates of the different reaction pathways, the individual stoichiometric reactions of the *n*-alkanes were quantitatively evaluated. Although monomolecular reactions prevailed in our experiments, we also considered the minor contributions of bimolecular pathways in order to fully close the mass balance.

Monomolecular α-cracking of *n*-alkanes leads to one paraffin molecule and one adsorbed carbenium ion (11). The surface-bound carbenium ion might (i) desorb as olefin, (ii) abstract a hydride ion from another saturated hydrocarbon (12, 14, 17–21), or (iii) react further by oligomerization and/or secondary β-cracking (12, 14, 19). If the carbenium ion desorbs as olefin, the paraffin to olefin (P/O) ratio in the products will be one. The formation of isoparaffins indicates hydride transfer, because the rate of isomerization of the olefins is high. In contrast, a P/O ratio smaller than one suggests secondary cracking of the carbenium ion to yield an olefin and a smaller carbenium ion. Because seconadary cracking of propene and butene requires primary carbenium ions, the probability of undergoing secondary cracking increases with the chain length of the olefin. Therefore, the P/O ratio decreases with increasing molecular weight (17). The concentration of olefins in the product stream is thus markedly influenced by the rate of secondary reactions.

At differential conversion, the rates of production or consumption r_i and the total rate r_{tot} (carbon balance) are described by

$$r_i = \frac{X_i \cdot \dot{V}}{m_{Cat}} \qquad [1]$$

$$r_{tot} = \frac{1}{n}\left[1 \cdot r_{C_1} + 2 \cdot \sum r_{C_2} + \cdots + n \cdot \sum r_{C_n} + \cdots + (n+x) \cdot \sum r_{C_{n+x}}\right]. \qquad [2]$$

X_i, $\dot{V}$ m_{Cat}, n, and x denote the individual conversion, the volumetric flow rate of the feed (mol/sec), the mass of the catalyst (g), the number of carbon atoms in the feed molecule, and a positive integer (denoting an increase in chain length), respectively. Four assumptions were made to account quantitatively for the reactions described above: (i) The rate of an individual primary cracking reaction (cleavage of one of the carbon–carbon bonds) is equal to the rate of formation of the corresponding alkane. The produced alkanes do not react further. The excess of the corresponding alkene was attributed to other reactions (e.g., β-cracking). (ii) The total rate of primary cracking is the sum of the individual reaction rates. (iii) The rate of dehydrogenation is equal to the rate of formation of the olefin with the same carbon number as the feed molecule plus the concentration of the olefins resulting from secondary cracking of these dehydrogenated products (i.e., the excess of olefins described under (i)). (iv) The sum of the rates of the different reaction pathways (cracking, dehydrogenation) equals the total rate.

RESULTS

The Rates of Hydrocarbon Conversion and the Order of Reaction

The rates of product formation are compiled in Table 1 for all hydrocarbons investigated. The rates of the individual reaction networks are listed in Tables 2–4. Please note that all rates were normalized to the corresponding partial pressures and are expressed in terms of mol · s^{-1} · g^{-1} · bar^{-1}. Turnover frequencies were calculated by normalizing these values to the concentration of strong Brønsted acid sites.

TABLE 1

Individual Rates of Product Formation for the Conversion of the Linear Hydrocarbons over H–ZSM-5 at 773 K (Rates × 10^6 (mol/g s bar))

	Propane	*n*-Butane	*n*-Pentane	*n*-Hexane
Methane	1.1	3.7	9.4	17
Ethane		3.6	20.9	54
Ethene	1.1	3.8	16.3	28
Propane	Feed		7.2	42
Propene	0.6	3.6	29.8	120
n-Butane		Feed	1.1	13
Butene isomers		2.7	8.4	56
n-Pentane			Feed	0.9
Pentene isomers			3.2	4
n-Hexane				Feed

TABLE 3

Reaction Network for the Conversion of *n*-Pentane over H–ZSM-5 at 773 K

No.	Reaction	Rates × 10^6 (mol/g s bar)	TOF × 10^3 (molecules/site s bar)
R1	$C_5H_{12} \rightarrow C_1 + C_4^{2-}$	9.4	22.4
R2	$C_5H_{12} \rightarrow C_2 + C_3^{2-}$	20.9	49.8
R3	$C_5H_{12} \rightarrow C_3 + C_2^{2-}$	7.2	17.1
R4	$C_5H_{12} \rightarrow H_2 + C_5^{2-}$	12.3	29.3
R5	$C_5^{2-} \rightarrow C_2^{2-} + C_3^{2-}$	9.1	21.7
	$r_{Cracking}$ (Σ R1, R2, R3)	37.5	89.3
	$r_{Dehydrogenation}$ (R4)	12.3	29.3
	$r_{Cracking} + r_{Dehydrogenation}$	49.8	118.6
	r_{Total} (Carbon balance)	49.8	118.6

The orders of the observed cracking reactions were unity for all hydrocarbons, indicating that monomolecular reactions prevailed under the experimental conditions applied. This is exemplified for *n*-pentane in Fig. 1. It should be especially emphasized that neither the selectivity nor the apparent energies of activation changed in the pressure interval reported. At higher pressures small amounts of isoparaffins indicated minor contributions of bimolecular reactions.

The dependence of the rates on the chain length is shown in Fig. 2. The rate of cracking increased exponentially from 1.1×10^{-6} for propane to 1.27×10^{-4} for *n*-hexane at 773 K. Similarly, the rates of dehydrogenation increased from 6.1×10^{-7} for propane to 4.1×10^{-5} for *n*-hexane. For all hydrocarbons the rate of cracking exceeded the rates of the other reactions.

The rates for the individual dehydrogenation reactions (i.e., the formation of propene from propane, butene from *n*-butane, etc.) are also compiled in Tables 1–4. The apparent selectivity to dehydrogenation decreased with increasing chain length of the hydrocarbon. This is primarily due to the increasing reactivity of olefins with higher molecular weight.

The apparent energies of activation for cracking decreased with increasing chain length of the hydrocarbon (see Table 5 and Fig. 3). In parallel, the heats of adsorption increased, indicating a constant true energy of activation for all alkanes. The selectivities observed for the cleavage of central and terminal carbon–carbon bonds (see below) did not change as a function of temperature, indicating the

TABLE 2

Reaction Network for the Conversion of *n*-Butane over H–ZSM-5 at 773 K

No.	Reaction	Rates × 10^6 (mol/g s bar)	TOF × 10^3 (molecules/site s bar)
R1	$C_4H_{10} \rightarrow C_1 + C_3^{2-}$	3.7	8.8
R2	$C_4H_{10} \rightarrow C_2 + C_2^{2-}$	3.6	8.6
R3	$C_4H_{10} \rightarrow H_2 + C_4^{2-}$	2.8	6.7
R4	$C_4^{2-} \rightarrow 2\ C_2^{2-}$	0.1	0.2
	$r_{Cracking}$ (Σ R1, R2)	7.3	17.4
	$r_{Dehydrogenation}$ (R3)	2.8	6.7
	$r_{Cracking} + r_{Dehydrogenation}$	10.1	24.1
	r_{Total} (Carbon balance)	10	23.8

TABLE 4

Reaction Network for the Conversion of *n*-Hexane over H–ZSM-5 at 773 K

No.	Reaction	Rates × 10^6 (mol/g s bar)	TOF × 10^3 (molecules/site s bar)
R1	$C_6H_{14} \rightarrow C_1 + C_5^{2-}$	17	41
R2	$C_6H_{14} \rightarrow C_2 + C_4^{2-}$	54	129
R3	$C_6H_{14} \rightarrow C_3 + C_3^{2-}$	42	100
R4	$C_6H_{14} \rightarrow C_4 + C_2^{2-}$	13	31
R5	$C_6H_{14} \rightarrow H_2 + C_6^{2-}$	32	76
R6	$C_6^{2-} \rightarrow C_3^{2-} + C_3^{2-}$	32	76
R7	$C_5^{2-} \rightarrow C_2^{2-} + C_3^{2-}$	14	33
	$r_{Cracking}$ (Σ R1, R2, R3, R4)	126	300
	$r_{Dehydrogenation}$ (R5)	32	76
	$r_{Cracking} + r_{Dehydrogenation}$	158	376
	r_{Total} (Carbon balance)	161	383

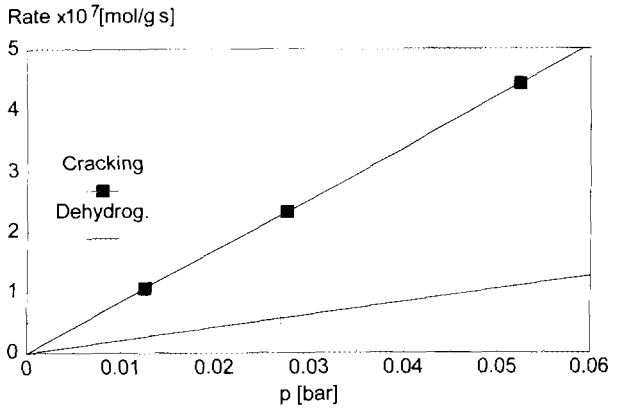

FIG. 1. Reaction order for cracking and dehydrogenation of *n*-pentane over H-ZSM-5 at 773 K.

same energy of activation for the protolytic cracking of all carbon–carbon bonds (see Fig. 4).

Reactions of Propane

Methane and ethene and hydrogen and propene were determined to be the primary products. This was concluded from the positive initial slopes of these products in a yield vs conversion plot. In addition, traces of ethane were found. Hydrocarbons with more than three carbon atoms were not detected. The sum of the rates of primary cracking and dehydrogenation equals the total rate, indicating that the mass balance was closed. Thus, the reaction products and rates observed can be well explained by protolytic cleavage of propane into methane and ethene as well as propene and hydrogen with nearly complete absence of hydride transfer and/or secondary cracking of the propene. It should be noted that the rates of formation of methane and ethene were higher than that for propene (see Table 1) and that these differences increased with temperature.

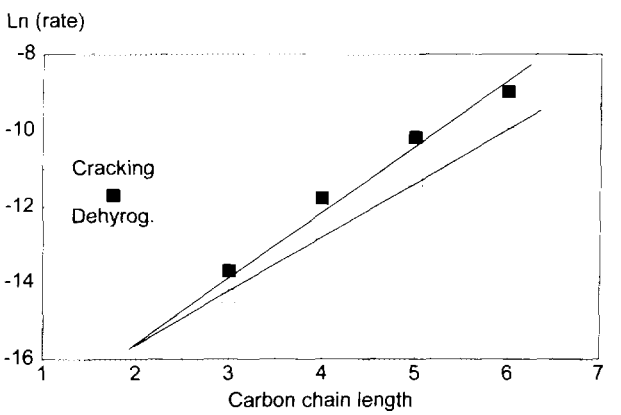

FIG. 2. Rates of cracking and dehydrogenation of linear hydrocarbons over H-ZSM-5 at 773 K vs the carbon chain length.

TABLE 5

Heats of Adsorption, Apparent and True Energies of Activation, Paraffin/Olefin Ratios and Cracking/Dehydrogenation Ratios for the Conversion of the *n*-Alkanes over H-ZSM-5 at 773 K

Reactant	Heat of adsorption (kJ/mol)	$E_{A\ app.\ Cracking}$ (kJ/mol)	$E_{A\ true\ Cracking}$ (kJ/mol)	P/O	C × 100 / (C + D)
Propane	43	155	198	0.7	65%
n-Butane	62	135	197	0.7	72%
n-Pentane	74	120	194	0.7	75%
n-Hexane	92	105	197	0.6	80%

The apparent energies of activation for cracking and dehydrogenation were 155 and 95 kJ/mol, respectively.

Reactions of n-Butane

The individual reaction pathways and their rates over H-ZSM-5 at 773 K are compiled in Table 2. The conversion of *n*-butane yielded methane and propene, and ethane and ethene in approximately equimolar amounts. Additionally, hydrogen and butene were formed. All these products were determined to be primary.

Ethene was observed in a small excess of ethane. This excess was quantitatively attributed to secondary cracking of butene isomers via formation of primary carbenium ions. The excess formation of ethene increased with increasing temperature. Formation of ethene via cracking of (di-)oligomerized butene is excluded, because propene was not observed in excess of the expected stoichiometric concentration and C_5 hydrocarbons were not detected.

As in the case of propane, cracking of *n*-butane exceeded the rate of dehydrogenation. However, cracking proceeded at approximately twice the rate of dehydrogenation, indicating a decrease in the importance of dehydrogenation compared to propane. The selectivities of the two individ-

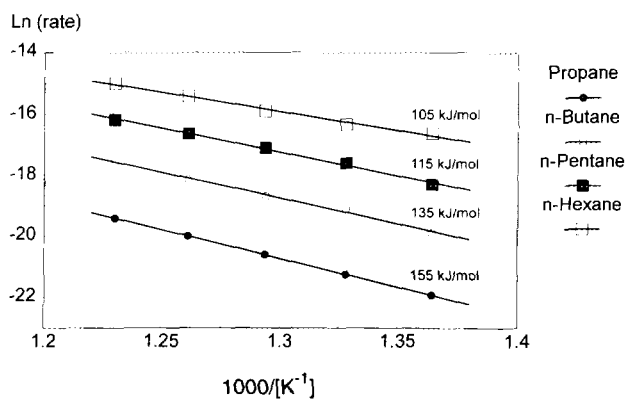

FIG. 3. Arrhenius plot for protolytic cracking of the *n*-alkanes.

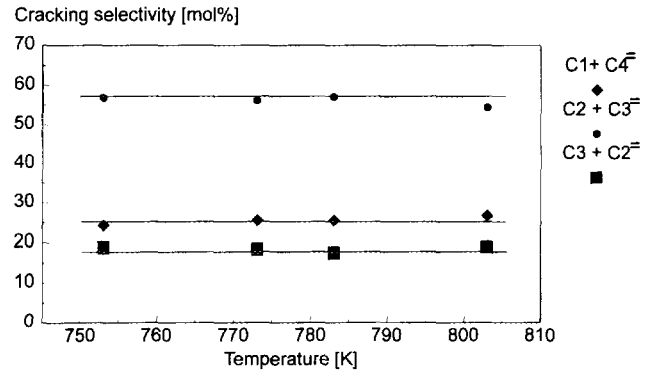

FIG. 4. Cracking selectivities upon conversion of *n*-pentane over H–ZSM-5 as a function of temperature.

ual cracking pathways, i.e., the formation of (i) methane and propene and (ii) ethane and ethene, did not change with temperature, indicating identical apparent energies of activation for the cleavage of all carbon–carbon bonds. However, the selectivity to dehydrogenation decreased with increasing temperature, indicating a lower energy of activation for dehydrogenation than for cracking. The apparent energies of activation were 135 kJ/mol for cracking and 115 kJ/mol for dehydrogenation. Hydrogen–deuterium exchange experiments indicated that the rate of protonation–deprotonation exceeds all other rates by at least one order of magnitude. The apparent energy of activation for this reaction was approximately 80 kJ/mol (16, 21).

The concentrations of the butene isomers were close to their thermodynamic equilibrium values, suggesting fast double bond, *cis/trans*, and skeletal isomerization. Propane and *i*-butane were observed in negligible concentrations between 723 and 823 K, indicating that hydrogen transfer plays only a minor role.

Reactions of n-Pentane

The individual reaction pathways of *n*-pentane conversion over H–ZSM-5 at 773 K and the corresponding rates are compiled in Table 3 and in Fig. 5. As for propane and *n*-butane, the product distribution could be well explained by monomolecular cracking. Methane and butene, ethane and propene, ethene and propane, and hydrogen and pentene were the primary reaction products.

While methane and butene were found in approximately equimolar concentrations, an excess of ethene over propane and of propene over ethane was detected. This was attributed to secondary cracking of pentene formed via dehydrogenation. The sum of the rate of pentene formation and the rates of excess alkene formation amounted to 25% of the total reaction rate. Thus, compared to propane and *n*-butane, a smaller contribution of the dehydrogenation to the overall conversion was observed.

Above 710 K, neither i-pentane nor *i*- and/or *n*-butane were detected in appreciable quantities, suggesting the absence of hydride transfer reactions. Below 710 K, the formation of *i*-pentane, and *n*- and *i*-butane was observed. In combination with the sudden absence of methane in the products, this indicates a rapid transition from the monomolecular to the bimolecular cracking mechanism (e.g., 19).

The selectivities within the cracking products did not change as a function of temperature, indicating the same energy of activation for the cleavage of all carbon–carbon bonds (see Fig. 4). The apparent energy of activation for cracking was determined to be 120 kJ/mol. Similar to the conversion of *n*-butane, the pentene isomers were detected in their equilibrium concentrations.

Reactions of n-Hexane

As for the smaller alkanes, the conversion of *n*-hexane over H–ZSM-5 between 723 and 803 K is fully explained by monomolecular reactions. The individual reaction pathways and the corresponding rates at 773 K are compiled in Table 4. Five major elementary reactions were considered to describe the reaction network of the *n*-hexane conversion: (i) Formation of methane and pentene isomers. The latter can desorb or crack further into ethene and propene. (ii) Formation of ethane and butenes in equimolar amounts. Under all experimental conditions, the butenes were present in their equilibrium composition. (iii) Formation of propene and propane. An excess of propene was formed, which was attributed to secondary cracking of pentyl- and hexyl-carbenium ions. (iv) Formation of ethene and *n*-butane. The excess of ethene over *n*-butane is attributed to the decomposition of the pentyl-carbenium ion into ethene and propene. Hexyl-carbenium ions decompose primarily to propene. (v) Dehydrogenation of *n*-

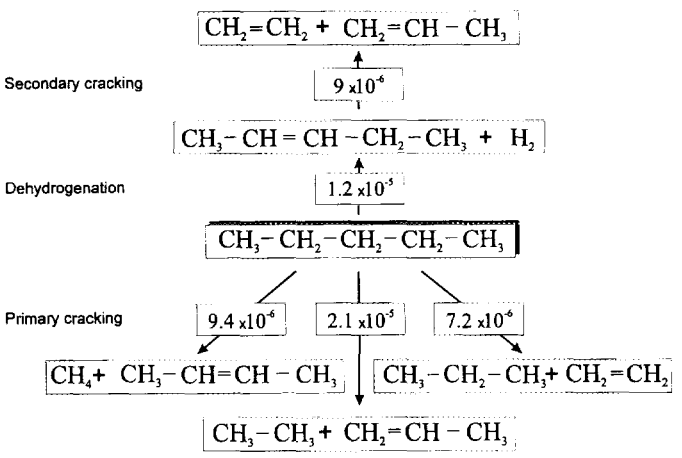

FIG. 5. Reaction network for *n*-pentane conversion over H–ZSM-5 at 773 K. Rates in mol/g s bar.

hexane to hexene, which is instantaneously cracked further, so that only traces of hexene were observed.

In accordance with the trend of decreasing importance of dehydrogenation with increasing size of the hydrocarbon the ratio of cracking to dehydrogenation was the highest for hexane compared to the other hydrocarbons studied. Again changes in the selectivities of the cracking products over the temperature range were not observed, suggesting an identical energy of activation for the cleavage of all carbon bonds. The apparent energy of activation for cracking was 105 kJ/mol.

DISCUSSION

The Reaction Mechanism

The product selectivities and the first-order pressure dependence indicate that alkane conversion can be described by monomolecular reactions. Although the contribution of primary reactions dominated, secondary cracking of the carbenium ions increased with alkane chain length. Hydride transfer was observed to set in only below 710 K.

The material studied did not show measurable concentrations of Lewis acid sites. Thus, strong Brønsted acidic hydroxyl groups are concluded to be the active sites. These hydroxyl groups interact with the alkanes via hydrogen bonding and generate pentacoordinated carbonium ions (11, 22–24) in the transition states.

Subsequently, three reactions are possible: (i) donation of the proton back to the zeolite (hydrogen exchange), (ii) cleavage of two carbon–hydrogen bonds to form hydrogen and a secondary carbenium ion (dehydrogenation), and (iii) breaking of a carbon–carbon bond to form an alkane and a primary carbenium ion (cracking). The apparent energies of activation increased in the sequence hydrogen exchange < dehydrogenation < cracking. The rates of these reactions increased, however, in the sequence dehydrogenation < cracking $\ll$ hydrogen exchange. We think that all three processes occur in a concerted manner, involving little charge separation. A schematic sketch of the transition state and the energetic pathways for *n*-butane is given in Fig. 6 (see also ref. (24)).

The adsorbed, hydrogen bonded *n*-alkane represents the common reaction precursor for all these primary processes. The protolytic cleavage of the carbon–carbon bonds initially leads to the formation of primary carbenium ions, while secondary carbocations are formed during dehydrogenation. Thus, the lower energy of activation for dehydrogenation may be explained by the Evans–Polanyi relation (25) correlating the higher enthalpies of primary carbenium ions with the higher energy of activation. The low selectivity to dehydrogenation then implies that the preexponential factor and thus the transition state entropy is lower for dehydrogenation than for cracking. This may be caused by the fact that the structure of the transition state is closer to the more tightly bound carbenium ion in alkane dehydrogenation than in cracking. Note that this strictly holds only for the light hydrocarbons (propane and butane) while the larger hydrocarbons undergo complex secondary reactions, causing a much higher energy of activation.

The highly endothermic nature of the formation of the carbonium ions suggests that they exist only as activated complexes in the transition state. Theoretical calculations (26–28) indicated it to be rather unlikely that these ions are stabilized as intermediates in the zeolite pores. The different energies of activation imply, therefore, separate reaction pathways for hydrogen exchange, cracking, and dehydrogenation. We conclude that protonation and bond cleavage occur in concerted steps (schematically depicted in Fig. 6). Whatever the absolute energy barrier may be for the two processes, we conclude that it is the transition state entropy and not the transition state enthalpy or the lifetime of the carbonium ion which determines the differences in the rates.

The Role of the Alkane Chain Length

As compiled in Table 5, the apparent energies of activation of cracking decreased with increasing chain length of the hydrocarbon. In the same sequence, the heats of adsorption (15) increased (see Fig. 7). This suggests a constant true energy of activation for the conversion of *n*-alkanes, independent of their chain length.

It was shown that the adsorption of *n*-alkanes on H-ZSM-5 can be described by a set of Langmuir isotherms (15). At high temperatures, low alkane coverages prevail. Under these conditions the adsorption can be described by a Langmuir isotherm in its reduced form, i.e., $\theta = K \cdot p$. Then, the apparent rate constants of the hydrocarbon reactions may be expressed as the product of the adsorption constant and the rate constant of the corresponding process.

As shown in Fig. 2, the rates of cracking and dehydrogenation followed an exponential increase with the chain length of the hydrocarbon. The corresponding adsorption equilibrium constants for the *n*-alkanes taken from Ref. (15) also showed an exponential increase with the chain length of the hydrocarbon. Thus, we conclude that it is primarily the sorption constant which influences the variation of the reaction rate.

The Selectivity of the Carbon–Carbon Bond Cleavage

The selectivity to cleave central carbon–carbon bonds increases with increasing chain length (see Tables 1–4). Because the selectivities to the cracked products were independent of the temperature (and hence the apparent energies of activation for the cleavage of central and terminal carbon–carbon bonds are identical) this is unlikely to be explained by weaker inner C—C bonds. Thus, we propose

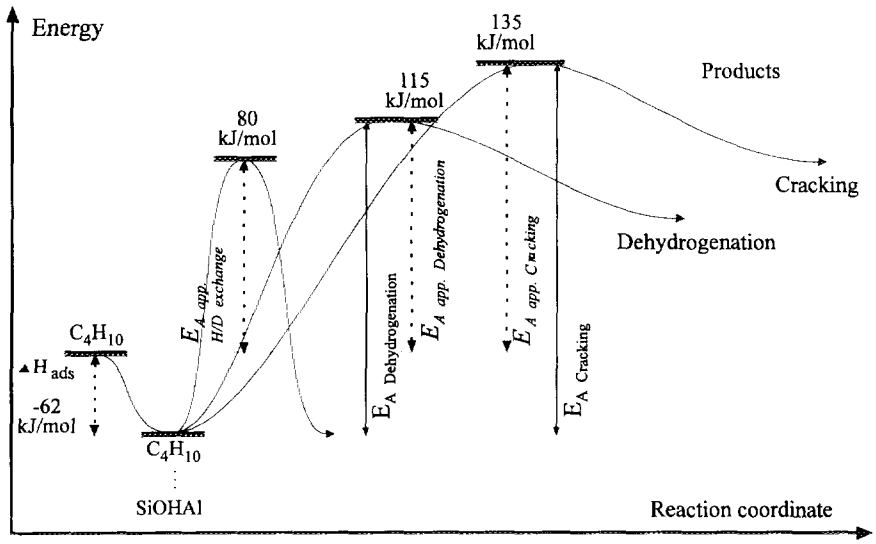

FIG. 6. Energy scheme for H/D exchange, monomolecular cracking, and dehydrogenation.

that the entropy of the sorbed state of the reactant and/or the transition state entropy control the selectivity. The tendency to crack the alkane in such a way that the largest possible carbenium ion is formed upon decomposition of a given carbonium ion supports this, as the larger carbenium ion will have a higher entropy in the transition state.

Secondary Reactions

Under the reaction conditions employed, skeletal isomerization and cracking of the olefins are secondary reactions. The contribution of the latter increased strongly with increasing chain length of the carbenium ion. The increased reactivity of the sorbed alkene is caused by two factors: (i) the increasing true residence time of the alkenes with increasing chain length (which is due to stronger interactions with the zeolites (26)) and (ii) the lower apparent energy of activation for the larger alkenes that can crack via secondary carbenium ions.

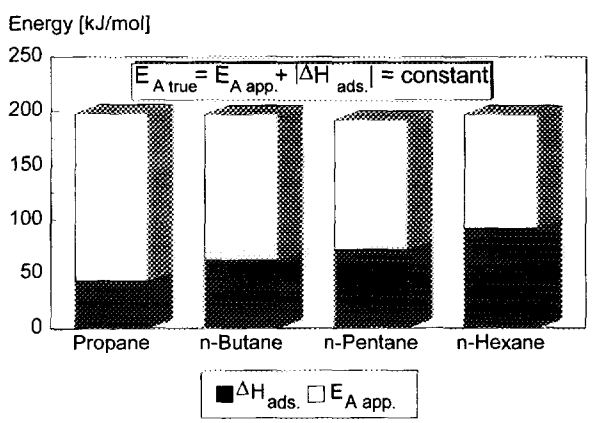

FIG. 7. Heats of adsorption and energies of activation for cracking of *n*-alkanes over H–ZSM-5.

CONCLUSIONS

The high-temperature conversion of light *n*-alkanes over H–ZSM-5 proceeds through two monomolecular reactions, i.e., cracking and dehydrogenation. In parallel, rapid protonation/deprotonation (H/D exchange) may occur, which does not lead to further reaction. The extent of secondary cracking depends upon the size of the carbenium ion, formed in the primary process, as well as upon the concentrations of the olefins present.

The true energy of activation for carbon–carbon bond cleavage is independent of (i) the chain length of the hydrocarbon and (ii) the position of the carbon–carbon bond. Therefore, the transition state entropy or the differences in sorption entropy must account for the different product selectivities.

The reaction rates for cracking and dehydrogenation increased exponentially with increasing carbon chain length. The same dependence was found for hydrocarbon sorption which led us to conclude that the activity depends primarily upon hydrocarbon adsorption. For all alkanes investigated, the rate of dehydrogenation was significantly smaller than the rate of cracking. The lower dehydrogenation activity compared to that of cracking suggests a significantly lower transition state entropy for the former reaction, i.e., an activated complex which is more tightly bound to the surface.

The importance of the secondary reactions was found to critically depend upon the type of carbenium ion in-

volved as intermediate in the corresponding process. When primary carbenium ions need to be formed for cracking, low rates were observed (as for propene and butene). When secondary carbenium ions can participate in the reaction route for cracking, higher secondary conversions were observed.

The observed results together with theoretical calculations suggest that the carbonium ions should be rather seen as transition states than as stable, high-energy intermediates (24, 26–28). In contrast, the carbenium ions are assumed to be formed as stable intermediates. Their surface concentration determines the extent of bimolecular reactions. The temperature, the size of the hydrocarbons, and the nature of the bonds involved in the stabilization of the carbocations will determine the residence time of the hydrocarbon on the acid site.

ACKNOWLEDGMENTS

The H-ZSM-5 sample was obtained from Dr. Werner Haag (Mobil Oil). The financial support of this work by the Christian Dopper Society is gratefully acknowledged.

REFERENCES

1. Jacobs, P. A., "Carboniogenic Activity of Zeolites." Elsevier, Amsterdam, 1977.
2. Venuto, P. B., and Habib, E. T., Jr., "Fluid Catalytic Cracking with Zeolite Catalysts." Dekker, New York, 1979.
3. Wojciechowski, B. W., and Corma, A., "Catalytic Cracking." Dekker, New York 1986.
4. Biswas, J., and Maxwell, I. E., *Appl. Catal.* **63,** 197 (1990).
5. Scherzer, J., *Catal. Rev. Sci. Eng.* **31**(3), 215 (1989).
6. Gates, B. C., Katzer, J. R., and Schuit, G. C. A., "Chemistry of Catalytic Processes." McGraw-Hill, New York, 1979.
7. Lombardo, E. A., and Hall, W. K., *J. Catal.* **112,** 565 (1988).
8. Lombardo, E. A., Gaffney, T. R., and Hall, W. K., *in* "Proceedings, 9th International Congress on Catalysis, Calgary, 1988" (M. J. Phillips and M. Ternan, Eds.), Vol. 1, p. 412. Chem. Institute of Canada, Ottawa, 1988.
9. Lombardo, E. A., Pierantozzi, R., and Hall, W. K., *J. Catal.* **110,** 171 (1988).
10. Auroux, A., Tuel, A., Bandiera, J., and Taarit, Y. B., *Appl. Catal.* **93,** 181 (1993).
11. Haag, W. O., Dessau, R. M., *in* "Proceedings, 8th International Congress on Catalysis Berlin, 1984." Vol. 2, p. 305. Dechema, Frankfurt-am-Main, 1984.
12. Abbot, J. and Wojciechowski, B. W., *Can. J. Chem. Eng.* **63,** 462 (1985).
13. Bolton, P., Ladd, I. R., and Weeks, T. J. J., *in* Proceedings, 6th International Congress on Catalysis, London, 1976" (G. C. Bond, P. B. Wells, and F. C. Tompkins, Eds.) The Chemical Society, London 1977.
14. Corma, A., Planelles, J., Sanchez-Marin, J., and Tomas, F., *J. Catal.* **93,** 30 (1985).
15. Stockenhuber, M., Thesis, Technical University of Vienna, 1994.
16. Narbeshuber, T. F., Thesis, University of Twente, ISBN 90-9007754-5, Enschede, The Netherlands, 1994.
17. Abbot, J., *Appl. Catal.* **57,** 105 (1990).
18. Rollmann, L. D., *J. Catal.* **49,** 113 (1977).
19. Zhao, Y., Bamwenda, G. R., Groten, W. A., and Wojciechowski, B. W., *J. Catal.* **140,** 243 (1993).
20. Corma, A., Fornes, V., Manton, J. B., and Orchilles, A. V., *Appl. Catal.* **12,** 105 (1984).
21. Narbeshuber, T. F., Brait, A., Seshan, K., and Lercher, J. A., submitted for publication.
22. Olah, G. A., Halpern, Y., Shen, J., and Mo, Y. K., *J. Am. Chem. Soc.* **95,** 4960 (1973).
23. Haag, W. O., Lago, R. M., and Weisz, P. B., *Faraday Discuss. Chem. Soc.* **72,** 317 (1982).
24. Lercher, J. A., van Santen, R. A., and Vinek, H., *Catal. Lett.* **27,** 91 (1994).
25. Dumesic, J. A., Rudd, D. F., Aparicio, L. M., Rekoske, J. E., and Treviño, A. A., *in* "The Microkinetics of Heterogeneous Catalysis." Am. Chem. Soc., Washington, DC, 1993.
26. Kazanskii, V. B., and Senchenya, I. W., *J. Catal.* **119,** 108 (1989).
27. Kazansky, V. B., Senchenya, I. N., Frash, M. V., and van Santen, R. A., *Catal. Lett.* **27,** 345 (1994).
28. Kazansky, V. B., Frash, M. V., and van Santen, R. A., *Catal. Lett.* **28,** 211 (1994).